# SOME NEW AIRFOILS

Richard Eppler
Universität Stuttgart
Stuttgart, West Germany

## SUMMARY

A computer approach to the design and analysis of airfoils and some common problems concerning laminar separation bubbles at different lift coefficients are discussed briefly. Examples of application to ultralight airplanes, canards, and sailplanes with flaps are given.

## INTRODUCTION

In the 1940's, NACA demonstrated clearly that it is possible to design airfoils from pressure distributions in such a way that the boundary layer would behave in a desired manner (Refs. 1 and 2). At that time, it was discovered that the boundary layer would remain laminar longer if the pressure minimum occurred further aft on the airfoil. This realization led to the first laminar airfoils. Since that time, better methods for designing airfoils from pressure distributions have been developed (Ref. 3). Simple methods for computing the characteristics of laminar and turbulent boundary layers including a feasible transition criterion have also been developed (Ref. 4). The occurrence of laminar separation bubbles has been detected and studied experimentally (Ref. 5) and correlated with theory (Ref. 4). Good methods for the analysis of the potential flow around a given airfoil have been developed (Ref. 6). Thus, it was possible to write computer programs which combine all of these methods. These programs allow airfoils to be designed with prescribed pressure-distribution properties, the boundary-layer characteristics to be determined, and the effects of shape modifications such as plain or variable geometry flap deflections to be analyzed. A complete description of such a program system will soon be published as a NASA technical memorandum (Eppler and Somers). This system is somewhat equivalent to a wind tunnel. Three fundamental differences do exist, however. First, the computer analysis of an airfoil is much less expensive than the corresponding wind-tunnel test. Second, the total time required to obtain the final results is much shorter. Third, much more data, such as development of the boundary-layer shape factor and thickness, are available. Moreover, the modification of an airfoil through prescribing the pressure distribution, which must be done on the computer, is integrated into the program system. This allows a boundary-layer development with prescribed properties to be obtained directly.

Thus, the time has come to use the computer when a new airfoil is to be developed. Wind-tunnel and flight tests should be used to obtain a better understanding of fundamental phenomena in support of the theory. Accordingly, an appropriate, or even an optimized, airfoil could be developed for each application rather than looking for an acceptable airfoil in an airfoil catalog. All such catalogs together could not cover all practical requirements. The Reynolds numbers, wing loadings, flaps, takeoff and landing requirements, structural constraints, moment restrictions, surface qualities, and many other specifications vary over wide ranges. It is not possible to develop catalogs for all such requirements. Only for a few applications, such as sailplanes with smooth surfaces and model airplanes, have catalogs been used successfully (Refs. 7 and 8). Even for these applications, new requirements arise which cannot be satisfied by existing airfoils. Other applications (e.g., general aviation, remotely piloted vehicles, and hydrofoil boats) are still far from having a list of standard requirements.

So, the tailoring of airfoils to specific applications becomes increasingly important. This paper presents some general considerations for tailoring airfoils and some examples of specific applications.

## GENERAL CONSIDERATIONS

Airfoil design means to specify an airfoil from its pressure distribution in such a way that the boundary layer behaves in a desired manner. This approach usually leads to certain problems. Some of these problems are briefly discussed in this section.

The velocity distribution over an airfoil changes with angle of attack. An example is given in Figure 1 which shows the velocity distributions of an airfoil at seven angles of attack. (Note that all velocity distributions in this paper are presented in terms of the ratio (V) of the local potential-flow velocity to the free-stream potential-flow velocity.) The differences between the different curves are nearly independent of the particular airfoil and are approximately proportional to the differences between the corresponding flat-plate velocity distributions. Normally the design of an airfoil means the specification of the entire velocity distribution at one angle of attack only. This is called a one-point design. The design method mentioned previously (Ref. 3), however, permits a multipoint design in which the velocities are specified along different segments of the airfoil at different angles of attack.

For Reynolds numbers below about $4 \times 10^6$, one of the most important problems concerns laminar separation bubbles which usually occur if transition takes place in an adverse pressure gradient. It is well known that this phenomenon can cause a substantial increase in the total drag (Ref. 5). This increase depends primarily on the Reynolds number R and the degree of adverse pressure gradient near transition. At lower Reynolds numbers, less adverse pressure gradient is allowed. A so-called "transition ramp" must be introduced ahead of the pressure recovery in order to obtain a fully developed, turbulent boundary layer. At Reynolds numbers below about $10^5$, a fully developed, turbulent boundary layer is not possible at all and, accordingly, the adverse pressure gradient can be only slightly steeper than the one which a laminar boundary layer could overcome without separating. The theory (Ref. 4) as used in the program system provides a certain bubble analog. If this analog is prevented, the real flow does not normally show an additional bubble drag.

The problems associated with laminar separation bubbles become more difficult as angle of attack changes. As shown in Figure 1, the transition ramp introduced on the upper surface at high angles of attack $\alpha$ is reduced and even eliminated at lower $\alpha$. For all multipoint designs, this problem is most difficult to solve. Fortunately, another effect helps the situation. For an airplane in flight, the Reynolds number changes with angle of attack or lift coefficient $c_l$. Thus, lower $c_l$ means higher velocity and correspondingly higher Reynolds number. This fact can be exploited by requiring a less steep transition ramp at lower $c_l$. On the upper surface, it is even possible to eliminate the transition ramp required at higher $c_l$ and, thereby, allow an extension of the laminar flow region at lower $c_l$ and higher R. On the lower surface, a laminar separation bubble and even separation of the turbulent boundary layer can be permitted at low $c_l$ and low R. As R increases to the free-flight value, the bubble and the turbulent separation should disappear. As $c_l$ increases, the adverse pressure gradient should be reduced to an amount suitable for a transition ramp.

All of these features are illustrated in Figure 2 which contains the theoretical section characteristics for the airfoil shown in Figure 1. This airfoil was designed for a sailplane. The Reynolds number corresponding to low $c_l$ is approximately $R = 3 \times 10^6$. The Reynolds number for high $c_l$ is about $R = 10^6$. For $c_l < 0.5$ and $R = 10^6$, which is not achievable in flight by the sailplane, turbulent boundary-layer separation was permitted on the lower surface. As $c_l$ is decreased from 1.2 to 0.6, the transition point on the upper surface moves aft approximately 10% of the chord because the transition ramp essentially "disappears."

Some unpublished wind-tunnel data (Althaus, Universität Stuttgart, 1975), and free-flight data (Ref. 9) are included in Figure 2. The latter data agree very well with the theory, while the wind-tunnel results show some discrepancies. The differences in transition point are inconsequential because a microphone was used in the wind tunnel to detect transition. This technique probably detects only a fully developed, turbulent boundary layer, and therefore, experimental points lay somewhat behind the theoretical ones. Of more importance are the differences among the drag polars. The wind-tunnel curve for $R = 10^6$ is characteristic of a polar for an airfoil with a small laminar separation bubble. That is to say that low drag is achieved at low and high, but not medium, lift coefficients. This problem was apparently not experienced in flight. Even more important are the drag differences for $c_l < 0.2$ and $R = 3 \times 10^6$. Here the free-flight tests indicate that the theoretical results are probably more reliable than those measured in the wind tunnel.

In summary, it is very likely that the "computer wind tunnel" can predict at least the differences between different airfoils so reliably that it should be used to design an airfoil for a specific application.

## AIRFOILS FOR ULTRALIGHT AIRPLANES

Ultralight airplanes usually have only one side of the airfoil covered. This means that the airfoil has essentially zero thickness. The structure is concentrated primarily near the leading edge and to a lesser extent near the trailing edge. The problem, then, is the sharp suction peak which occurs near the leading edge at all off-design conditions. A high maximum lift coefficient $c_{l_{max}}$ and a soft stall are desirable for takeoff and landing, whereas because of the low aspect ratio, the lift coefficient for minimum sinking speed as well as for maximum glide ratio is usually somewhat less than $c_{l_{max}}$. Good penetration at even lower $c_l$ is also sometimes desired. Thus, the problem is to design thin airfoils exhibiting a range of lift coefficient over which the flow is not entirely separated. Some thickness is, of course, required near the leading edge for structure. The following examples demonstrate what can be achieved by carefully shaping the leading-edge region. The first example, airfoil 379, is shown in Figure 3 along with its velocity distributions. At $\alpha = 7^o$ relative to the zero-lift direction, a very high suction peak has already occurred on the lower surface near the leading edge. On the upper surface, a suction peak forms as $\alpha$ increases but the $\Delta V_{max}/\Delta\alpha$ is much less than for the lower surface. The pressure recovery is slightly concave, but by no means as severe as the recovery typical of the Stratford distribution. This shallow, concave pressure recovery together with the rounded, upper-surface suction peak results in a soft stall which is most important for the application.

The section characteristics for this airfoil are shown in Figure 4. A high maximum lift and a soft stall are achieved, but below $c_l = 1.0$, the lower-surface flow is separated. The separation is predicted at about x/c = 0.8. This is a consequence of the assumption that the flow will reattach in a favorable gradient which, in this case, is probably not true. Thus, the flow on the lower surface must be considered separated from the leading edge aft.

An attempt to lower the lower-surface, leading-edge suction peak is shown in Figure 5. This airfoil, 378, is much thicker than the previous one (3.88% versus 2.10%). As shown in Figure 6, lower-surface separation is now predicted below $c_l = 0.6$, and thus, a much wider range of lift coefficient is available.

Figures 7 and 8 show airfoil 377, which is similar to 378 except that it is shifted to a higher lift coefficient.. Using the design method mentioned above, this is easily accomplished.

The lower surface of this airfoil was then modified so that "zero" thickness was reached at a more forward x/c. The new shape and its velocity distribution are shown in Figure 9 and an overlay of Figures 7 and 9 is presented in Figure 10. Notice that the lower-surface flow exhibits much more adverse pressure gradient after the modification. As a consequence, the flow on the lower surface for this case is separated at all lift coefficients. This demonstrates the danger involved in arbitrarily modifying an airfoil to a shape which only looks appropriate.

Airfoil 376 was designed to have the same upper-surface behavior as airfoil 377 but to have less thickness and reach zero thickness at about x/c = 0.25 (Fig. 11). This airfoil has a maximum thickness of 2.21%. It has a certain $c_l$ range over which the flow is not separated, and hence, is much better than airfoil 377 modified (Fig. 12). This range is still considerably less than that for the original airfoil 377.

These five examples illustrate the possibilities for thin airfoils. Many other constraints probably exist and, therefore, more tailoring would be required for this application.

Another category of ultralight airplanes is becoming more popular, the so-called foot-launched sailplane with an empty weight of around 45 kg, full controls, and an enclosed cockpit. This concept was demonstrated in the 1930's when the "Windspiel" was built. Today's materials allow much more efficient structures than were available at that time.

The airfoil requirements for this application include high maximum lift coefficient, soft stall, and low drag down to $c_l \approx 0$. Because of the low wing loadings involved, penetration always means low $c_l$. Airfoil 748 (Fig. 13) was tailored for this application which covers a Reynolds number range from 0.6 x $10^6$ to 3 x $10^6$ (Fig. 14). This airfoil requires a smooth surface for the forward 45% of the chord. If this can be accomplished, an aircraft with much lower wing loading than, say, a Ka-6 or Schweizer 1-26 can achieve the penetration of these heavier sailplanes and yet have a minimum speed which would permit simple takeoff procedures including foot-launch from a ridge with little wind.

## AIRFOILS FOR CANARDS

Because of longitudinal-stability requirements, a canard (forward wing) must always operate at a higher $c_l$ than the main (rear) wing. The maximum lift coefficient of the main wing is, therefore, constrained by the $c_{l_{max}}$ of the canard. Thus, it would be senseless to incorporate lift-increasing devices on the main wing if none were included on the canard. Fortunately, the canard usually includes an elevator which is deflected down to obtain higher $c_l$ from the main wing. Thus, the elevator acts as a lift-increasing device for the canard. This effect, however, does depend on center-of-gravity position. The design objectives of airfoils for canards, therefore, include high $c_{l_{max}}$ with small downward flap deflection, low drag at low $c_l$ with no flap deflection, and a certain thickness for structural reasons. The Reynolds numbers are relatively low because of the small chord lengths.

Two examples illustrate this application. The velocity distributions for the first example, airfoil 1230, are shown in Figure 15. The upper surface is designed only for high $c_{l_{max}}$. This is accomplished by preventing suction peaks and by including a certain transition ramp. Even at low $c_l$, only 20% of the upper surface can sustain laminar flow. The lower surface can have about

50% laminar flow. The theoretical section characteristics are shown in Figure 16. For positive flap deflection (down), some problems exist at low $c_l$. This combination, however, cannot occur in flight. The second example, airfoil 1233 (Fig. 17), achieves even higher $c_{l_{max}}$ (Fig 18). This airfoil is also thicker, and therefore, a drag penalty is paid at low $c_l$. The lower surface of this airfoil can sustain only 30% laminar flow. An airfoil between these two examples has been successfully applied on Burt Rutan's "Defiant" (Ref. 10).

## AIRFOILS FOR SAILPLANES WITH FLAPS

Sailplanes with normally hinged flaps are a standard application of airfoils. The difficulties with this application come from two requirements. First, the flap-down case usually corresponds to a Reynolds number of $10^6$ or below. For this case, laminar separation bubbles can be dangerous. This danger is increased by the steep adverse pressure gradient immediately downstream of the suction peak at the flap hinge. Second, the negative-flap-deflection (up) case corresponds to $R > 3 \times 10^6$. For this case, transition can occur earlier than desired. For a zero pressure gradient at these Reynolds numbers, the boundary layer is not stable enough to remain laminar for 60% to 70% of the surface and, therefore, a certain favorable pressure gradient is necessary to keep the boundary layer laminar.

Airfoil 662 was designed for this application. The velocity distributions for this airfoil with flap deflections ($\beta$) of $0^\circ$, $10^\circ$ (down), and $-7.5^\circ$ (up) are shown in Figure 19. The pressure recovery on the upper surface for the undeflected-flap case must be less than would be possible for the case where no flap deflections were intended. A flap deflection in either direction increases the amount of adverse pressure gradient. Severe separation would occur in these cases if the pressure recovery for the undeflected case were already approaching the separation limit. The flap deflection can, however, be exploited in a favorable sense as well. For the flap-down case, a distinct transition ramp forms between the original pressure recovery and the suction peak caused by the flap. On the lower surface, an additional favorable pressure gradient occurs with the flap up which stabilizes the laminar boundary layer at the higher Reynolds numbers. Attention to all of these details together with the careful designing of the leading-edge region results in the good performance illustrated in Figure 20. Notice that, at low $c_l$ and low R, a lower-surface separation was again permitted.

Another application resulted from the practical achievement of the variable-geometry concept. A flap which extends the chord 20% while introducing essentially no disturbances in the flap-retracted configuration was developed by F. Mahrer and incorporated into his sailplane, "Delphin" (Ref. 11). This flap could only be applied over that portion of the span which required no aileron. It was, therefore, desirable to deflect the ailerons down for the high-lift case. A negative flap deflection was not allowed. Thus, an airfoil was required which would have a laminar bucket that would extend down to around $c_l = 0.05$ and which would achieve a high $c_{l_{max}}$ with a plain and a variable-geometry flap.

The velocity distributions for such an airfoil, 664, are shown in Figure 21. The transition ramp between the original pressure recovery and the flap hinge is again exploited for the flap-down case. The favorable pressure gradient aft of $x/c = 0.5$, however, had to be introduced for this airfoil because no flap-up deflection was possible. The section characteristics for this airfoil are shown in Figure 22.

## CONCLUSIONS

Some new airfoils have been designed for specific applications through the use of a computer program. The applications included ultralight airplanes, canards, and sailplanes with flaps. The coordinates, moment coefficients, and zero-lift angles for all the airfoils presented are given as an appendix. The tailoring of airfoils should be encouraged because it is highly unlikely that airfoil catalogs will be produced for all possible applications. The reliability of this theoretical approach increases as more wind-tunnel and flight-test data are correlated with the theory. So far, many such theoretically developed airfoils have been successfully applied.

## APPENDIX

## COORDINATES, MOMENT COEFFICIENTS, AND ZERO-LIFT ANGLES FOR VARIOUS AIRFOILS

PROFIL 376 2.21%

| N | X | Y |
|---|---|---|
| 0 | 100.000 | 0.000 |
| 1 | 99.712 | .036 |
| 2 | 98.849 | .145 |
| 3 | 97.421 | .333 |
| 4 | 95.449 | .614 |
| 5 | 92.973 | .991 |
| 6 | 90.032 | 1.458 |
| 7 | 86.668 | 2.006 |
| 8 | 82.930 | 2.627 |
| 9 | 78.865 | 3.308 |
| 10 | 74.528 | 4.036 |
| 11 | 69.976 | 4.794 |
| 12 | 65.266 | 5.566 |
| 13 | 60.459 | 6.330 |
| 14 | 55.616 | 7.067 |
| 15 | 50.796 | 7.746 |
| 16 | 46.060 | 8.335 |
| 17 | 41.448 | 8.787 |
| 18 | 36.977 | 9.073 |
| 19 | 32.667 | 9.180 |
| 20 | 28.535 | 9.106 |
| 21 | 24.597 | 8.851 |
| 22 | 20.866 | 8.433 |
| 23 | 17.362 | 7.879 |
| 24 | 14.119 | 7.217 |
| 25 | 11.168 | 6.463 |
| 26 | 8.532 | 5.640 |
| 27 | 6.235 | 4.767 |
| 28 | 4.289 | 3.865 |
| 29 | 2.708 | 2.960 |
| 30 | 1.493 | 2.078 |
| 31 | .646 | 1.255 |
| 32 | .154 | .528 |
| 33 | .001 | -.032 |
| 34 | .208 | -.294 |
| 35 | .853 | -.209 |
| 36 | 2.019 | .261 |
| 37 | 3.812 | 1.147 |
| 38 | 6.345 | 2.430 |
| 39 | 9.745 | 4.025 |
| 40 | 14.128 | 5.792 |
| 41 | 19.602 | 7.425 |
| 42 | 25.964 | 8.437 |
| 43 | 32.615 | 8.690 |
| 44 | 39.205 | 8.452 |
| 45 | 45.654 | 7.935 |
| 46 | 51.910 | 7.233 |
| 47 | 57.925 | 6.433 |
| 48 | 63.663 | 5.586 |
| 49 | 69.093 | 4.739 |
| 50 | 74.180 | 3.910 |
| 51 | 78.885 | 3.126 |
| 52 | 83.174 | 2.404 |
| 53 | 87.016 | 1.763 |
| 54 | 90.386 | 1.213 |
| 55 | 93.264 | .767 |
| 56 | 95.632 | .433 |
| 57 | 97.496 | .219 |
| 58 | 98.864 | .095 |
| 59 | 99.712 | .026 |
| 60 | 100.000 | -.000 |

CM= -.1197 $\beta$= 5.97°

PROFIL 377 3.63%

| N | X | Y |
|---|---|---|
| 0 | 100.000 | 0.000 |
| 1 | 99.709 | .039 |
| 2 | 98.840 | .157 |
| 3 | 97.407 | .363 |
| 4 | 95.434 | .664 |
| 5 | 92.957 | 1.060 |
| 6 | 90.015 | 1.545 |
| 7 | 86.650 | 2.112 |
| 8 | 82.909 | 2.751 |
| 9 | 78.841 | 3.449 |
| 10 | 74.501 | 4.193 |
| 11 | 69.944 | 4.966 |
| 12 | 65.229 | 5.751 |
| 13 | 60.416 | 6.527 |
| 14 | 55.567 | 7.272 |
| 15 | 50.741 | 7.959 |
| 16 | 45.998 | 8.553 |
| 17 | 41.379 | 9.006 |
| 18 | 36.901 | 9.292 |
| 19 | 32.584 | 9.397 |
| 20 | 28.446 | 9.316 |
| 21 | 24.503 | 9.054 |
| 22 | 20.766 | 8.625 |
| 23 | 17.259 | 8.059 |
| 24 | 14.014 | 7.381 |
| 25 | 11.062 | 6.611 |
| 26 | 8.428 | 5.767 |
| 27 | 6.134 | 4.871 |
| 28 | 4.196 | 3.945 |
| 29 | 2.625 | 3.013 |
| 30 | 1.428 | 2.102 |
| 31 | .602 | 1.244 |
| 32 | .136 | .482 |
| 33 | .010 | -.102 |
| 34 | .324 | -.406 |
| 35 | 1.141 | -.443 |
| 36 | 2.442 | -.204 |
| 37 | 4.290 | .363 |
| 38 | 6.755 | 1.263 |
| 39 | 9.928 | 2.461 |
| 40 | 13.876 | 3.866 |
| 41 | 18.637 | 5.342 |
| 42 | 24.199 | 6.713 |
| 43 | 30.484 | 7.754 |
| 44 | 37.233 | 8.211 |
| 45 | 44.016 | 8.077 |
| 46 | 50.591 | 7.580 |
| 47 | 56.901 | 6.879 |
| 48 | 62.899 | 6.056 |
| 49 | 68.544 | 5.179 |
| 50 | 73.800 | 4.292 |
| 51 | 78.634 | 3.436 |
| 52 | 83.016 | 2.639 |
| 53 | 86.923 | 1.926 |
| 54 | 90.333 | 1.316 |
| 55 | 93.231 | .821 |
| 56 | 95.607 | .456 |
| 57 | 97.474 | .226 |
| 58 | 98.849 | .100 |
| 59 | 99.707 | .028 |
| 60 | 100.000 | -.000 |

CM= -.1291 $\beta$= 6.08°

PROFIL 377
LOWER SURFACE CHANGED

| N | X | Y |
|---|---|---|
| 0 | 100.000 | 0.000 |
| 1 | 99.710 | .040 |
| 2 | 98.841 | .159 |
| 3 | 97.407 | .363 |
| 4 | 95.434 | .664 |
| 5 | 92.957 | 1.060 |
| 6 | 90.015 | 1.545 |
| 7 | 86.650 | 2.112 |
| 8 | 82.909 | 2.751 |
| 9 | 78.841 | 3.449 |
| 10 | 74.501 | 4.193 |
| 11 | 69.944 | 4.966 |
| 12 | 65.229 | 5.751 |
| 13 | 60.416 | 6.527 |
| 14 | 55.567 | 7.272 |
| 15 | 50.741 | 7.959 |
| 16 | 45.998 | 8.553 |
| 17 | 41.379 | 9.006 |
| 18 | 36.901 | 9.292 |
| 19 | 32.584 | 9.397 |
| 20 | 28.446 | 9.316 |
| 21 | 24.503 | 9.054 |
| 22 | 20.766 | 8.625 |
| 23 | 17.259 | 8.059 |
| 24 | 14.014 | 7.381 |
| 25 | 11.062 | 6.611 |
| 26 | 8.428 | 5.767 |
| 27 | 6.134 | 4.871 |
| 28 | 4.196 | 3.945 |
| 29 | 2.625 | 3.013 |
| 30 | 1.428 | 2.102 |
| 31 | .602 | 1.244 |
| 32 | .136 | .482 |
| 33 | .010 | -.102 |
| 34 | .324 | -.406 |
| 35 | 1.141 | -.443 |
| 36 | 2.442 | -.204 |
| 37 | 4.290 | .363 |
| 38 | 6.500 | 1.250 |
| 39 | 8.758 | 2.431 |
| 40 | 11.227 | 3.916 |
| 41 | 14.000 | 5.500 |
| 42 | 17.176 | 6.882 |
| 43 | 20.770 | 7.930 |
| 44 | 24.500 | 8.550 |
| 45 | 28.450 | 8.820 |
| 46 | 32.634 | 8.860 |
| 47 | 36.956 | 8.713 |
| 48 | 41.380 | 8.410 |
| 49 | 46.100 | 7.964 |
| 50 | 50.844 | 7.411 |
| 51 | 55.570 | 6.770 |
| 52 | 60.486 | 6.027 |
| 53 | 65.291 | 5.249 |
| 54 | 69.940 | 4.470 |
| 55 | 74.539 | 3.692 |
| 56 | 78.878 | 2.950 |
| 57 | 82.910 | 2.250 |
| 58 | 86.668 | 1.597 |
| 59 | 90.029 | 1.058 |
| 60 | 92.960 | .660 |
| 61 | 95.452 | .391 |
| 62 | 97.423 | .212 |
| 63 | 98.849 | .093 |
| 64 | 99.711 | .023 |
| 65 | 100.000 | 0.000 |

CM= -.1080 $\beta$=6.20°

# APPENDIX

PROFIL 378 3.88%

| N | X | Y |
|---|---|---|
| 0 | 100.000 | 0.000 |
| 1 | 99.707 | .024 |
| 2 | 98.827 | .100 |
| 3 | 97.362 | .240 |
| 4 | 95.333 | .469 |
| 5 | 92.783 | .797 |
| 6 | 89.760 | 1.219 |
| 7 | 86.308 | 1.727 |
| 8 | 82.476 | 2.312 |
| 9 | 78.318 | 2.964 |
| 10 | 73.888 | 3.670 |
| 11 | 69.247 | 4.413 |
| 12 | 64.455 | 5.177 |
| 13 | 59.574 | 5.940 |
| 14 | 54.668 | 6.680 |
| 15 | 49.798 | 7.368 |
| 16 | 45.027 | 7.968 |
| 17 | 40.394 | 8.430 |
| 18 | 35.916 | 8.726 |
| 19 | 31.611 | 8.841 |
| 20 | 27.496 | 8.772 |
| 21 | 23.586 | 8.521 |
| 22 | 19.892 | 8.105 |
| 23 | 16.435 | 7.554 |
| 24 | 13.248 | 6.894 |
| 25 | 10.362 | 6.144 |
| 26 | 7.801 | 5.325 |
| 27 | 5.586 | 4.457 |
| 28 | 3.734 | 3.563 |
| 29 | 2.255 | 2.666 |
| 30 | 1.153 | 1.795 |
| 31 | .426 | .985 |
| 32 | .064 | .285 |
| 33 | .055 | -.201 |
| 34 | .521 | -.423 |
| 35 | 1.528 | -.424 |
| 36 | 3.027 | -.172 |
| 37 | 5.074 | .378 |
| 38 | 7.733 | 1.224 |
| 39 | 11.076 | 2.329 |
| 40 | 15.155 | 3.606 |
| 41 | 19.995 | 4.932 |
| 42 | 25.572 | 6.148 |
| 43 | 31.813 | 7.052 |
| 44 | 38.466 | 7.414 |
| 45 | 45.133 | 7.232 |
| 46 | 51.587 | 6.724 |
| 47 | 57.777 | 6.038 |
| 48 | 63.657 | 5.253 |
| 49 | 69.190 | 4.428 |
| 50 | 74.339 | 3.607 |
| 51 | 79.073 | 2.825 |
| 52 | 83.363 | 2.110 |
| 53 | 87.186 | 1.481 |
| 54 | 90.522 | .956 |
| 55 | 93.356 | .545 |
| 56 | 95.678 | .259 |
| 57 | 97.504 | .105 |
| 58 | 98.856 | .043 |
| 59 | 99.707 | .013 |
| 60 | 100.000 | -.000 |

CM= -.1012 $\beta$= 5.02°

PROFIL 379 2.10%

| N | X | Y |
|---|---|---|
| 0 | 100.000 | 0.000 |
| 1 | 99.707 | .020 |
| 2 | 98.827 | .085 |
| 3 | 97.364 | .214 |
| 4 | 95.339 | .428 |
| 5 | 92.795 | .739 |
| 6 | 89.779 | 1.143 |
| 7 | 86.335 | 1.632 |
| 8 | 82.511 | 2.200 |
| 9 | 78.361 | 2.834 |
| 10 | 73.942 | 3.522 |
| 11 | 69.312 | 4.250 |
| 12 | 64.531 | 5.000 |
| 13 | 59.662 | 5.751 |
| 14 | 54.768 | 6.481 |
| 15 | 49.911 | 7.162 |
| 16 | 45.152 | 7.757 |
| 17 | 40.531 | 8.217 |
| 18 | 36.065 | 8.513 |
| 19 | 31.772 | 8.632 |
| 20 | 27.668 | 8.570 |
| 21 | 23.767 | 8.329 |
| 22 | 20.081 | 7.926 |
| 23 | 16.630 | 7.390 |
| 24 | 13.447 | 6.749 |
| 25 | 10.562 | 6.022 |
| 26 | 7.999 | 5.228 |
| 27 | 5.779 | 4.388 |
| 28 | 3.916 | 3.524 |
| 29 | 2.419 | 2.662 |
| 30 | 1.292 | 1.827 |
| 31 | .529 | 1.060 |
| 32 | .116 | .400 |
| 33 | .009 | -.066 |
| 34 | .282 | -.106 |
| 35 | 1.162 | .240 |
| 36 | 2.710 | .884 |
| 37 | 4.946 | 1.820 |
| 38 | 7.946 | 2.997 |
| 39 | 11.768 | 4.325 |
| 40 | 16.471 | 5.630 |
| 41 | 21.948 | 6.646 |
| 42 | 27.930 | 7.227 |
| 43 | 34.165 | 7.412 |
| 44 | 40.492 | 7.251 |
| 45 | 46.771 | 6.826 |
| 46 | 52.900 | 6.209 |
| 47 | 58.806 | 5.488 |
| 48 | 64.446 | 4.714 |
| 49 | 69.778 | 3.935 |
| 50 | 74.764 | 3.176 |
| 51 | 79.368 | 2.468 |
| 52 | 83.559 | 1.825 |
| 53 | 87.308 | 1.269 |
| 54 | 90.592 | .806 |
| 55 | 93.393 | .449 |
| 56 | 95.695 | .204 |
| 57 | 97.510 | .079 |
| 58 | 98.857 | .033 |
| 59 | 99.707 | .012 |
| 60 | 100.000 | -.000 |

CM= -.0822 $\beta$= 4.88°

PROFIL 748 19.73%

| N | X | Y |
|---|---|---|
| 0 | 100.000 | 0.000 |
| 1 | 99.641 | .122 |
| 2 | 98.632 | .505 |
| 3 | 97.102 | 1.131 |
| 4 | 95.133 | 1.899 |
| 5 | 92.723 | 2.711 |
| 6 | 89.835 | 3.545 |
| 7 | 86.485 | 4.425 |
| 8 | 82.726 | 5.357 |
| 9 | 78.615 | 6.330 |
| 10 | 74.212 | 7.330 |
| 11 | 69.581 | 8.340 |
| 12 | 64.785 | 9.335 |
| 13 | 59.887 | 10.290 |
| 14 | 54.948 | 11.177 |
| 15 | 50.028 | 11.967 |
| 16 | 45.180 | 12.630 |
| 17 | 40.456 | 13.136 |
| 18 | 35.901 | 13.453 |
| 19 | 31.541 | 13.546 |
| 20 | 27.392 | 13.402 |
| 21 | 23.468 | 13.018 |
| 22 | 19.779 | 12.401 |
| 23 | 16.337 | 11.577 |
| 24 | 13.164 | 10.572 |
| 25 | 10.282 | 9.417 |
| 26 | 7.714 | 8.142 |
| 27 | 5.482 | 6.781 |
| 28 | 3.606 | 5.368 |
| 29 | 2.104 | 3.939 |
| 30 | .992 | 2.534 |
| 31 | .284 | 1.201 |
| 32 | .000 | .006 |
| 33 | .275 | -.985 |
| 34 | 1.174 | -1.865 |
| 35 | 2.614 | -2.728 |
| 36 | 4.542 | -3.540 |
| 37 | 6.925 | -4.279 |
| 38 | 9.731 | -4.932 |
| 39 | 12.923 | -5.485 |
| 40 | 16.454 | -5.923 |
| 41 | 20.278 | -6.224 |
| 42 | 24.342 | -6.362 |
| 43 | 28.592 | -6.284 |
| 44 | 33.026 | -5.899 |
| 45 | 37.743 | -5.174 |
| 46 | 42.826 | -4.217 |
| 47 | 48.237 | -3.189 |
| 48 | 53.855 | -2.189 |
| 49 | 59.567 | -1.259 |
| 50 | 65.278 | -.434 |
| 51 | 70.888 | .248 |
| 52 | 76.292 | .759 |
| 53 | 81.380 | 1.084 |
| 54 | 86.044 | 1.220 |
| 55 | 90.181 | 1.180 |
| 56 | 93.695 | .984 |
| 57 | 96.483 | .673 |
| 58 | 98.462 | .338 |
| 59 | 99.621 | .090 |
| 60 | 100.000 | -.000 |

CM= -.1732 $\beta$= 6.65°

PROFIL 1230 17.46%

| N | X | Y |
|---|---|---|
| 0 | 100.000 | 0.000 |
| 1 | 99.850 | .039 |
| 2 | 99.418 | .167 |
| 3 | 98.742 | .396 |
| 4 | 97.859 | .715 |
| 5 | 96.797 | 1.095 |
| 6 | 95.562 | 1.503 |
| 7 | 94.141 | 1.915 |
| 8 | 92.517 | 2.331 |
| 9 | 90.691 | 2.765 |
| 10 | 88.676 | 3.221 |
| 11 | 86.484 | 3.699 |
| 12 | 84.128 | 4.199 |
| 13 | 81.622 | 4.720 |
| 14 | 78.980 | 5.258 |
| 15 | 76.219 | 5.812 |
| 16 | 73.353 | 6.378 |
| 17 | 70.399 | 6.950 |
| 18 | 67.373 | 7.524 |
| 19 | 64.290 | 8.094 |
| 20 | 61.167 | 8.655 |
| 21 | 58.019 | 9.200 |
| 22 | 54.861 | 9.722 |
| 23 | 51.708 | 10.214 |
| 24 | 48.574 | 10.671 |
| 25 | 45.472 | 11.085 |
| 26 | 42.415 | 11.449 |
| 27 | 39.414 | 11.758 |
| 28 | 36.482 | 12.005 |
| 29 | 33.627 | 12.186 |
| 30 | 30.860 | 12.294 |
| 31 | 28.190 | 12.325 |
| 32 | 25.623 | 12.274 |
| 33 | 23.166 | 12.138 |
| 34 | 20.823 | 11.911 |
| 35 | 18.594 | 11.591 |
| 36 | 16.479 | 11.180 |
| 37 | 14.478 | 10.683 |
| 38 | 12.591 | 10.105 |
| 39 | 10.817 | 9.454 |
| 40 | 9.157 | 8.744 |
| 41 | 7.618 | 7.987 |
| 42 | 6.206 | 7.191 |
| 43 | 4.928 | 6.366 |
| 44 | 3.787 | 5.521 |
| 45 | 2.789 | 4.665 |
| 46 | 1.937 | 3.807 |
| 47 | 1.236 | 2.958 |
| 48 | .688 | 2.129 |

PROFIL 1230 17.46%

| N | X | Y |
|---|---|---|
| 49 | .560 | 2.054 |
| 50 | .217 | 1.209 |
| 51 | .035 | .415 |
| 52 | .021 | -.302 |
| 53 | .231 | -.913 |
| 54 | .702 | -1.465 |
| 55 | 1.401 | -2.010 |
| 56 | 2.299 | -2.536 |
| 57 | 3.390 | -3.029 |
| 58 | 4.672 | -3.483 |
| 59 | 6.142 | -3.900 |
| 60 | 7.792 | -4.279 |
| 61 | 9.613 | -4.621 |
| 62 | 11.595 | -4.925 |
| 63 | 13.724 | -5.187 |
| 64 | 15.990 | -5.404 |
| 65 | 18.381 | -5.572 |
| 66 | 20.883 | -5.686 |
| 67 | 23.484 | -5.735 |
| 68 | 26.178 | -5.706 |
| 69 | 28.964 | -5.592 |
| 70 | 31.844 | -5.391 |
| 71 | 34.818 | -5.103 |
| 72 | 37.887 | -4.731 |
| 73 | 41.054 | -4.285 |
| 74 | 44.315 | -3.782 |
| 75 | 47.662 | -3.238 |
| 76 | 51.083 | -2.671 |
| 77 | 54.562 | -2.098 |
| 78 | 58.079 | -1.536 |
| 79 | 61.613 | -.997 |
| 80 | 65.141 | -.496 |
| 81 | 68.639 | -.043 |
| 82 | 72.081 | .352 |
| 83 | 75.441 | .681 |
| 84 | 78.691 | .939 |
| 85 | 81.804 | 1.122 |
| 86 | 84.754 | 1.229 |
| 87 | 87.513 | 1.261 |
| 88 | 90.056 | 1.223 |
| 89 | 92.358 | 1.118 |
| 90 | 94.390 | .953 |
| 91 | 96.124 | .746 |
| 92 | 97.538 | .524 |
| 93 | 98.627 | .317 |
| 94 | 99.394 | .149 |
| 95 | 99.850 | .039 |
| 96 | 100.000 | -.000 |

CM= -.1769 $\beta$= 7.01°

PROFIL 1233 19.38%

| N | X | Y |
|---|---|---|
| 0 | 100.000 | 0.000 |
| 1 | 99.855 | .051 |
| 2 | 99.438 | .214 |
| 3 | 98.791 | .497 |
| 4 | 97.954 | .880 |
| 5 | 96.952 | 1.329 |
| 6 | 95.787 | 1.807 |
| 7 | 94.442 | 2.290 |
| 8 | 92.898 | 2.778 |
| 9 | 91.154 | 3.284 |
| 10 | 89.224 | 3.813 |
| 11 | 87.119 | 4.364 |
| 12 | 84.850 | 4.935 |
| 13 | 82.432 | 5.526 |
| 14 | 79.878 | 6.133 |
| 15 | 77.202 | 6.752 |
| 16 | 74.419 | 7.380 |
| 17 | 71.545 | 8.011 |
| 18 | 68.594 | 8.640 |
| 19 | 65.582 | 9.262 |
| 20 | 62.525 | 9.870 |
| 21 | 59.437 | 10.458 |
| 22 | 56.332 | 11.020 |
| 23 | 53.226 | 11.548 |
| 24 | 50.132 | 12.036 |
| 25 | 47.063 | 12.477 |
| 26 | 44.032 | 12.864 |
| 27 | 41.050 | 13.192 |
| 28 | 38.129 | 13.454 |
| 29 | 35.278 | 13.644 |
| 30 | 32.509 | 13.757 |
| 31 | 29.830 | 13.787 |
| 32 | 27.246 | 13.727 |
| 33 | 24.761 | 13.575 |
| 34 | 22.379 | 13.328 |
| 35 | 20.102 | 12.985 |
| 36 | 17.929 | 12.549 |
| 37 | 15.863 | 12.025 |
| 38 | 13.904 | 11.418 |
| 39 | 12.053 | 10.736 |
| 40 | 10.312 | 9.991 |
| 41 | 8.688 | 9.195 |
| 42 | 7.186 | 8.357 |
| 43 | 5.814 | 7.486 |
| 44 | 4.576 | 6.589 |
| 45 | 3.478 | 5.676 |
| 46 | 2.524 | 4.757 |
| 47 | 1.717 | 3.839 |
| 48 | 1.061 | 2.934 |

PROFIL 1233 19.38%

| N | X | Y |
|---|---|---|
| 49 | .296 | 1.331 |
| 50 | .066 | .581 |
| 51 | .002 | -.103 |
| 52 | .126 | -.675 |
| 53 | .507 | -1.165 |
| 54 | 1.154 | -1.641 |
| 55 | 2.015 | -2.102 |
| 56 | 3.077 | -2.538 |
| 57 | 4.334 | -2.937 |
| 58 | 5.789 | -3.294 |
| 59 | 7.441 | -3.613 |
| 60 | 9.284 | -3.898 |
| 61 | 11.309 | -4.152 |
| 62 | 13.505 | -4.378 |
| 63 | 15.860 | -4.575 |
| 64 | 18.361 | -4.745 |
| 65 | 20.997 | -4.887 |
| 66 | 23.753 | -5.000 |
| 67 | 26.617 | -5.084 |
| 68 | 29.574 | -5.139 |
| 69 | 32.610 | -5.162 |
| 70 | 35.711 | -5.153 |
| 71 | 38.861 | -5.110 |
| 72 | 42.045 | -5.031 |
| 73 | 45.249 | -4.910 |
| 74 | 48.460 | -4.739 |
| 75 | 51.674 | -4.516 |
| 76 | 54.884 | -4.239 |
| 77 | 58.083 | -3.912 |
| 78 | 61.264 | -3.537 |
| 79 | 64.419 | -3.116 |
| 80 | 67.547 | -2.648 |
| 81 | 70.660 | -2.150 |
| 82 | 73.749 | -1.654 |
| 83 | 76.791 | -1.186 |
| 84 | 79.759 | -.762 |
| 85 | 82.626 | -.395 |
| 86 | 85.364 | -.093 |
| 87 | 87.944 | .137 |
| 88 | 90.340 | .294 |
| 89 | 92.524 | .380 |
| 90 | 94.468 | .397 |
| 91 | 96.144 | .357 |
| 92 | 97.530 | .278 |
| 93 | 98.612 | .183 |
| 94 | 99.384 | .092 |
| 95 | 99.846 | .025 |
| 96 | 100.000 | -.000 |

CM= -.1079 $\beta$= 4.88°

APPENDIX

PROFIL 662 15.02%

| N | X | Y |
|---|---|---|
| 0 | 100.000 | 0.000 |
| 1 | 99.642 | .118 |
| 2 | 98.640 | .483 |
| 3 | 97.117 | 1.056 |
| 4 | 95.113 | 1.745 |
| 5 | 92.609 | 2.516 |
| 6 | 89.626 | 3.395 |
| 7 | 86.231 | 4.390 |
| 8 | 82.500 | 5.493 |
| 9 | 78.528 | 6.682 |
| 10 | 74.435 | 7.890 |
| 11 | 70.276 | 8.968 |
| 12 | 65.983 | 9.824 |
| 13 | 61.519 | 10.489 |
| 14 | 56.922 | 10.988 |
| 15 | 52.232 | 11.331 |
| 16 | 47.501 | 11.525 |
| 17 | 42.776 | 11.570 |
| 18 | 38.108 | 11.470 |
| 19 | 33.541 | 11.225 |
| 20 | 29.121 | 10.841 |
| 21 | 24.891 | 10.324 |
| 22 | 20.891 | 9.681 |
| 23 | 17.159 | 8.923 |
| 24 | 13.729 | 8.062 |
| 25 | 10.631 | 7.113 |
| 26 | 7.892 | 6.094 |
| 27 | 5.535 | 5.024 |
| 28 | 3.578 | 3.926 |
| 29 | 2.037 | 2.828 |
| 30 | .921 | 1.761 |
| 31 | .239 | .770 |
| 32 | .003 | -.074 |
| 33 | .351 | -.733 |
| 34 | 1.336 | -1.289 |
| 35 | 2.879 | -1.785 |
| 36 | 4.966 | -2.210 |
| 37 | 7.571 | -2.567 |
| 38 | 10.668 | -2.858 |
| 39 | 14.221 | -3.088 |
| 40 | 18.189 | -3.264 |
| 41 | 22.522 | -3.392 |
| 42 | 27.165 | -3.474 |
| 43 | 32.061 | -3.512 |
| 44 | 37.148 | -3.506 |
| 45 | 42.363 | -3.456 |
| 46 | 47.642 | -3.357 |
| 47 | 52.919 | -3.206 |
| 48 | 58.130 | -2.993 |
| 49 | 63.214 | -2.702 |
| 50 | 68.116 | -2.302 |
| 51 | 72.841 | -1.742 |
| 52 | 77.449 | -1.061 |
| 53 | 81.940 | -.382 |
| 54 | 86.229 | .169 |
| 55 | 90.177 | .509 |
| 56 | 93.628 | .611 |
| 57 | 96.423 | .500 |
| 58 | 98.431 | .276 |
| 59 | 99.613 | .077 |
| 60 | 100.000 | -.000 |

CM= -.1497 $\beta$= 5.92°

PROFIL 664 16.63%

| N | X | Y |
|---|---|---|
| 0 | 100.000 | 0.000 |
| 1 | 99.623 | .092 |
| 2 | 98.557 | .391 |
| 3 | 96.923 | .881 |
| 4 | 94.774 | 1.491 |
| 5 | 92.110 | 2.193 |
| 6 | 88.964 | 3.005 |
| 7 | 85.407 | 3.927 |
| 8 | 81.512 | 4.942 |
| 9 | 77.353 | 6.020 |
| 10 | 73.008 | 7.122 |
| 11 | 68.549 | 8.197 |
| 12 | 64.043 | 9.167 |
| 13 | 59.497 | 9.937 |
| 14 | 54.869 | 10.482 |
| 15 | 50.167 | 10.840 |
| 16 | 45.437 | 11.029 |
| 17 | 40.727 | 11.060 |
| 18 | 36.087 | 10.938 |
| 19 | 31.564 | 10.670 |
| 20 | 27.205 | 10.262 |
| 21 | 23.051 | 9.720 |
| 22 | 19.145 | 9.055 |
| 23 | 15.521 | 8.277 |
| 24 | 12.216 | 7.401 |
| 25 | 9.258 | 6.441 |
| 26 | 6.674 | 5.416 |
| 27 | 4.487 | 4.348 |
| 28 | 2.714 | 3.261 |
| 29 | 1.371 | 2.183 |
| 30 | .468 | 1.155 |
| 31 | .023 | .229 |
| 32 | .146 | -.521 |
| 33 | .903 | -1.173 |
| 34 | 2.234 | -1.817 |
| 35 | 4.097 | -2.423 |
| 36 | 6.471 | -2.979 |
| 37 | 9.334 | -3.482 |
| 38 | 12.651 | -3.936 |
| 39 | 16.380 | -4.341 |
| 40 | 20.474 | -4.693 |
| 41 | 24.882 | -4.990 |
| 42 | 29.552 | -5.229 |
| 43 | 34.429 | -5.406 |
| 44 | 39.452 | -5.522 |
| 45 | 44.556 | -5.572 |
| 46 | 49.678 | -5.546 |
| 47 | 54.754 | -5.433 |
| 48 | 59.719 | -5.219 |
| 49 | 64.512 | -4.867 |
| 50 | 69.117 | -4.322 |
| 51 | 73.561 | -3.567 |
| 52 | 77.909 | -2.623 |
| 53 | 82.219 | -1.637 |
| 54 | 86.399 | -.808 |
| 55 | 90.260 | -.224 |
| 56 | 93.641 | .102 |
| 57 | 96.395 | .198 |
| 58 | 98.400 | .142 |
| 59 | 99.602 | .045 |
| 60 | 100.000 | -.000 |

CM= -.0908 $\beta$= 3.85°

PROFIL 664
VARIABLE GEOMETRY

| N | X | Y |
|---|---|---|
| 0 | 120.000 | -9.000 |
| 1 | 119.373 | -8.620 |
| 2 | 117.500 | -7.496 |
| 3 | 114.391 | -5.708 |
| 4 | 110.000 | -3.500 |
| 5 | 107.054 | -2.294 |
| 6 | 103.709 | -1.132 |
| 7 | 100.000 | 0.000 |
| 8 | 96.923 | .881 |
| 9 | 92.110 | 2.193 |
| 10 | 85.407 | 3.927 |
| 11 | 81.512 | 4.942 |
| 12 | 77.353 | 6.020 |
| 13 | 73.008 | 7.122 |
| 14 | 68.549 | 8.197 |
| 15 | 64.043 | 9.167 |
| 16 | 59.497 | 9.937 |
| 17 | 54.869 | 10.482 |
| 18 | 50.167 | 10.840 |
| 19 | 45.437 | 11.029 |
| 20 | 40.727 | 11.060 |
| 21 | 36.087 | 10.938 |
| 22 | 31.564 | 10.670 |
| 23 | 27.205 | 10.262 |
| 24 | 23.051 | 9.720 |
| 25 | 19.145 | 9.055 |
| 26 | 15.521 | 8.277 |
| 27 | 12.216 | 7.401 |
| 28 | 9.258 | 6.441 |
| 29 | 6.674 | 5.416 |
| 30 | 4.487 | 4.348 |
| 31 | 2.714 | 3.261 |
| 32 | 1.371 | 2.183 |
| 33 | .468 | 1.155 |
| 34 | .023 | .229 |
| 35 | .146 | -.521 |
| 36 | .903 | -1.173 |
| 37 | 2.234 | -1.817 |
| 38 | 4.097 | -2.423 |
| 39 | 6.471 | -2.979 |
| 40 | 9.334 | -3.482 |
| 41 | 12.651 | -3.936 |
| 42 | 16.380 | -4.341 |
| 43 | 20.474 | -4.693 |
| 44 | 24.882 | -4.990 |
| 45 | 29.552 | -5.229 |
| 46 | 34.429 | -5.406 |
| 47 | 39.452 | -5.522 |
| 48 | 44.556 | -5.572 |
| 49 | 49.678 | -5.546 |
| 50 | 54.754 | -5.433 |
| 51 | 59.719 | -5.219 |
| 52 | 64.512 | -4.867 |
| 53 | 69.117 | -4.322 |
| 54 | 74.184 | -3.641 |
| 55 | 79.152 | -3.041 |
| 56 | 84.000 | -2.650 |
| 57 | 88.180 | -2.542 |
| 58 | 92.188 | -2.639 |
| 59 | 96.000 | -2.900 |
| 60 | 100.411 | -3.401 |
| 61 | 104.421 | -4.078 |
| 62 | 108.000 | -4.900 |
| 63 | 112.280 | -6.177 |
| 64 | 115.631 | -7.351 |
| 65 | 118.047 | -8.254 |
| 66 | 119.510 | -8.812 |
| 67 | 120.000 | -9.000 |

## REFERENCES


1. Abbott, Ira H.; Von Doenhoff, Albert E.; and Stivers, Louis S., Jr.: Summary of Airfoil Data. NACA Rep. 824, 1945.

2. Abbott, Ira H.; and Von Doenhoff, Albert E.: Theory of Wing Sections. Dover Publications, Inc., 1959.

3. Eppler, R.: Direct Calculation of Airfoils From Pressure Distribution. NASA TT F-15417, 1974.

4. Eppler, R.: Practical Calculation of Laminar and Turbulent Bled-Off Boundary Layers. NASA TM-75328, 1978.

5. Wortmann, F. X.: Über den Ablösewinkel laminarer Ablöseblasen. Beiträge zur Strömungsmechanik und Flugmechanik, DLR-FB 74-62, 1974, pp. 10-1 - 10-13.

6. Hess, John L.: The Use of Higher-Order Surface Singularity Distributions To Obtain Improved Potential Flow Solutions for Two-Dimensional Lifting Airfoils. Computer Methods in Applied Mechanics and Engineering, vol. 5, no. 1, Jan. 1975, pp. 11-35.

7. Althaus, D.: MeBergebnisse aus dem Laminarwindkanal des Instituts für Aerodynamik und Fasdynamik der Universität Stuttgart. Stuttgarter Profilkatalog I, Institut für Aerodynamik und Gasdynamik der Universität Stuttgart, 1972.

8. Eppler,Profile. Verlag für Technik und Handwerk (Baden-Baden, Germany), 1977.

9. McMasters, J. H.: Low-Speed Drag Estimation Procedure Applied to the Astir CS Sailplane. Boeing Document D6-46968TN, Boeing, Jan. 1979.

10. Garrison, Peter: Rutan's Defiant. Flying, vol. 103, no. 6, Dec. 1978, pp. 55-59 and 86.

11. Wyler, Ruedi: Spaltenlose Fowlerklappen bie Segelflugzeugen. Aero Revue, Feb. 1979, pp. 75-77.

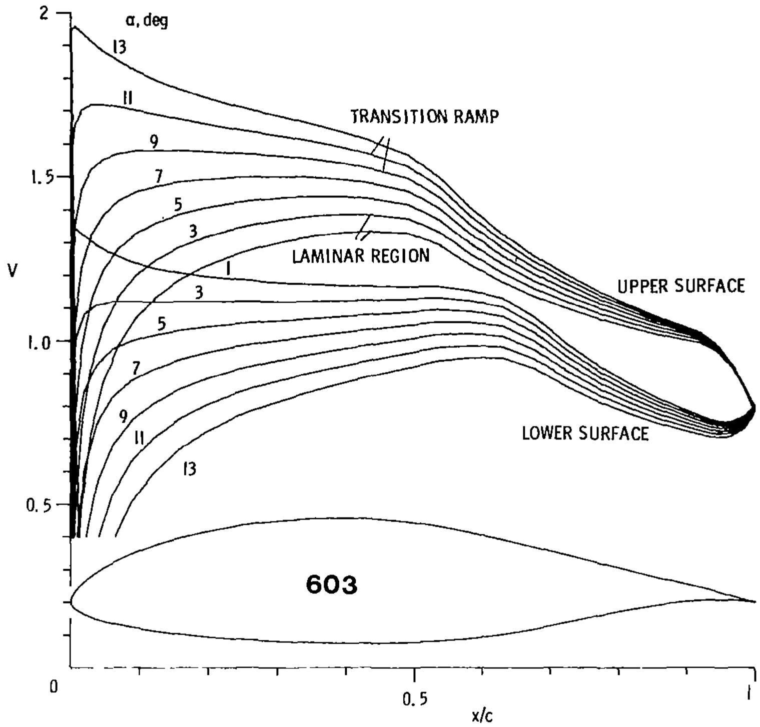


Figure 1.- Velocity distributions for airfoil 603.
α relative to zero-lift direction.

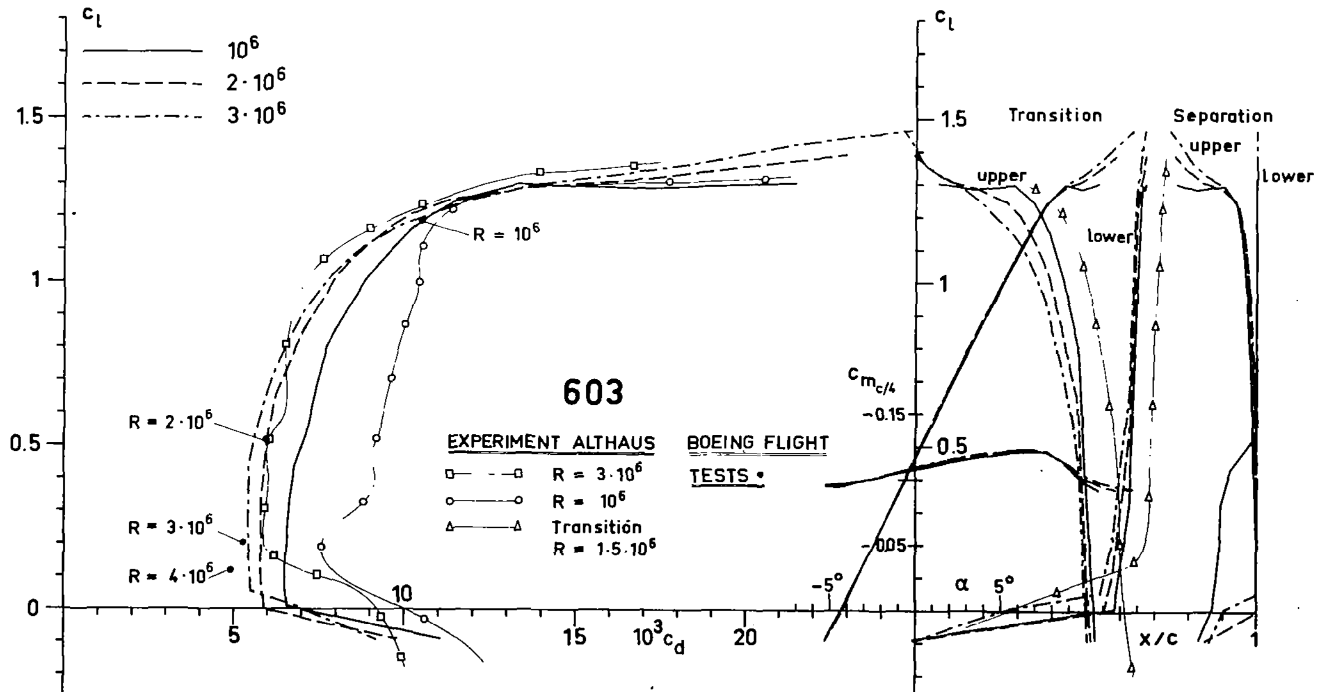


Figure 2.- Section characteristics for airfoil 603.

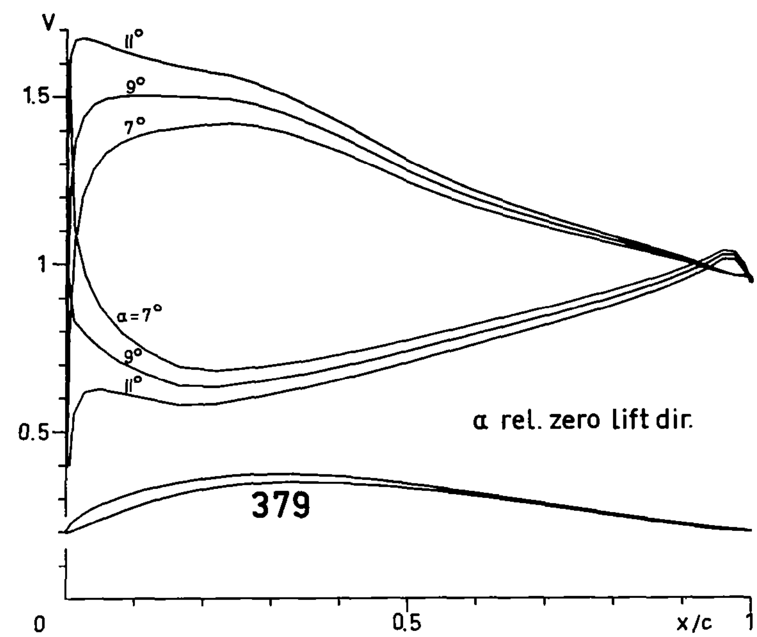


Figure 3.- Velocity distributions for airfoil 379.

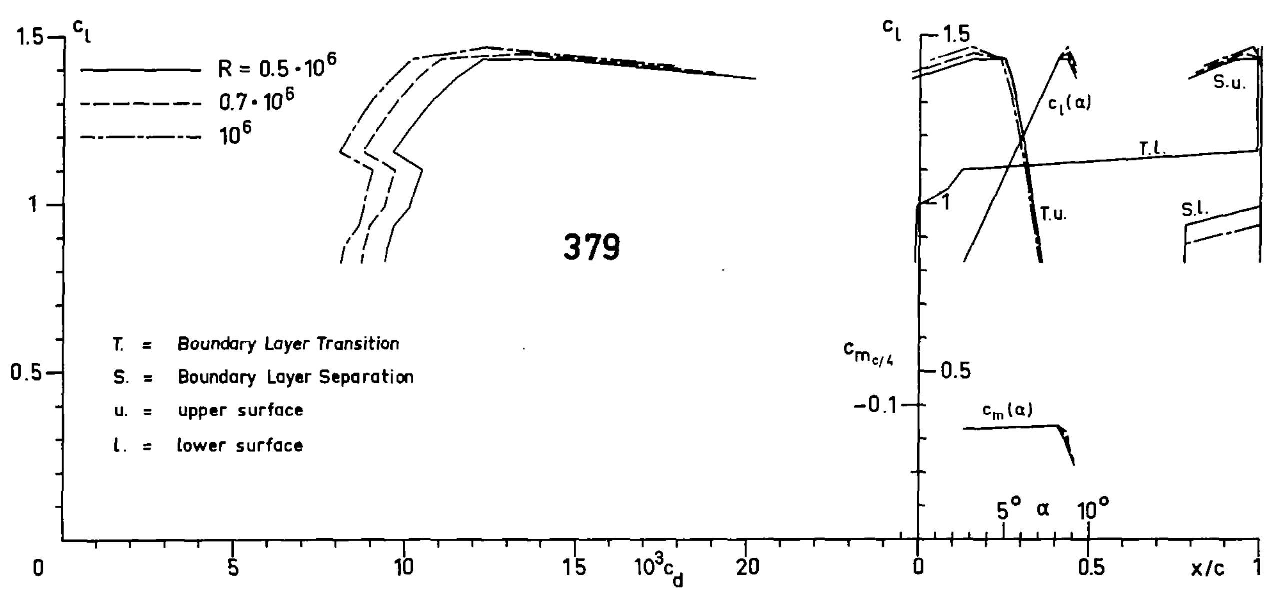


Figure 4.- Theoretical section characteristics for airfoil 379.

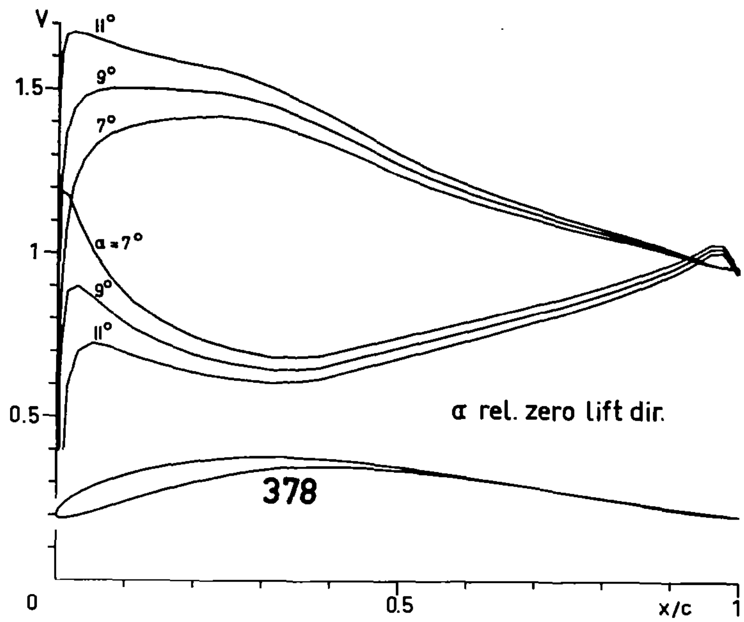


Figure 5.- Velocity distributions for airfoil 378.

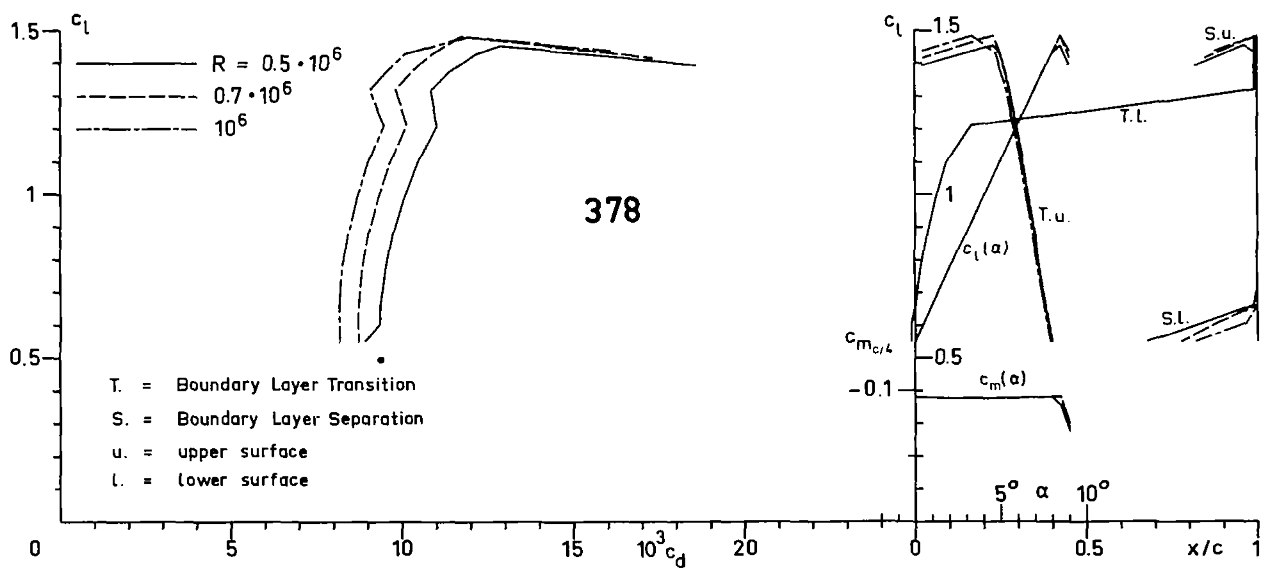


Figure 6.- Theoretical section characteristics for airfoil 378.

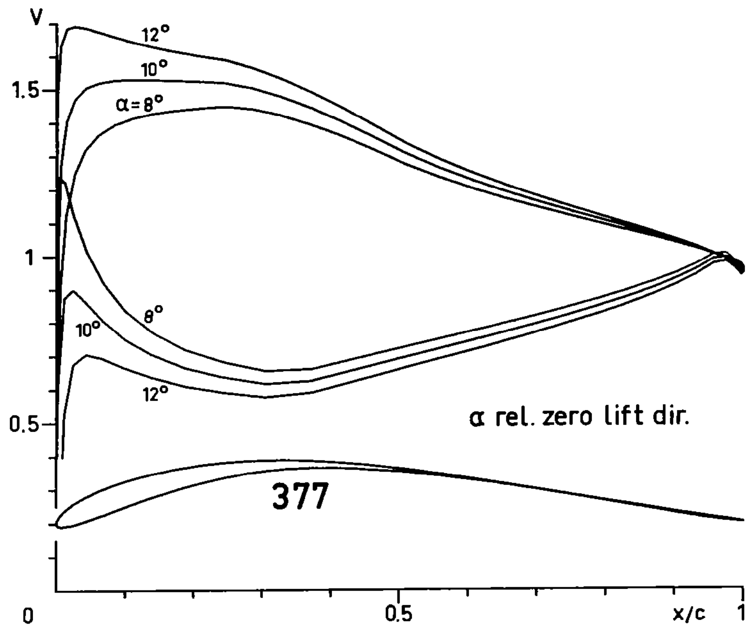


Figure 7.- Velocity distributions for airfoil 377.

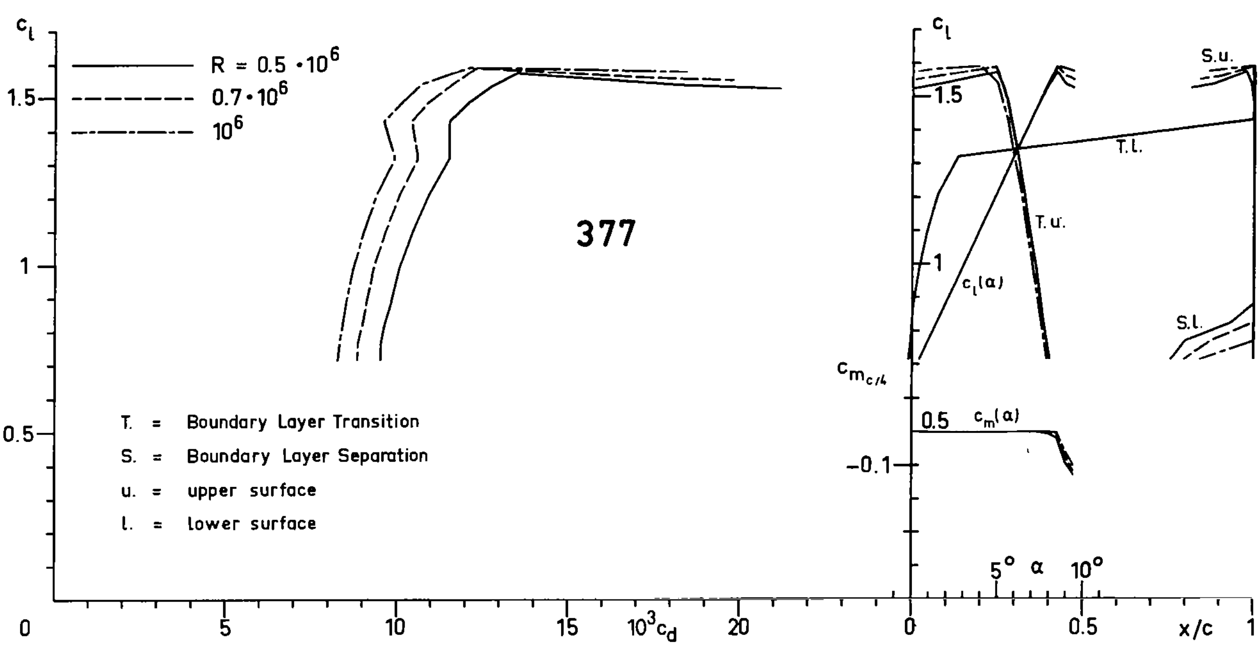


Figure 8.- Theoretical section characteristics for airfoil 377.

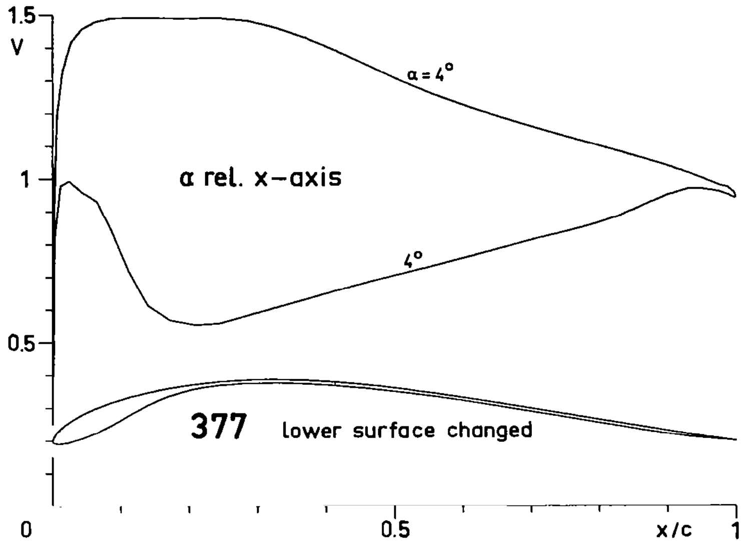


Figure 9.- Velocity distribution for airfoil 377 modified.

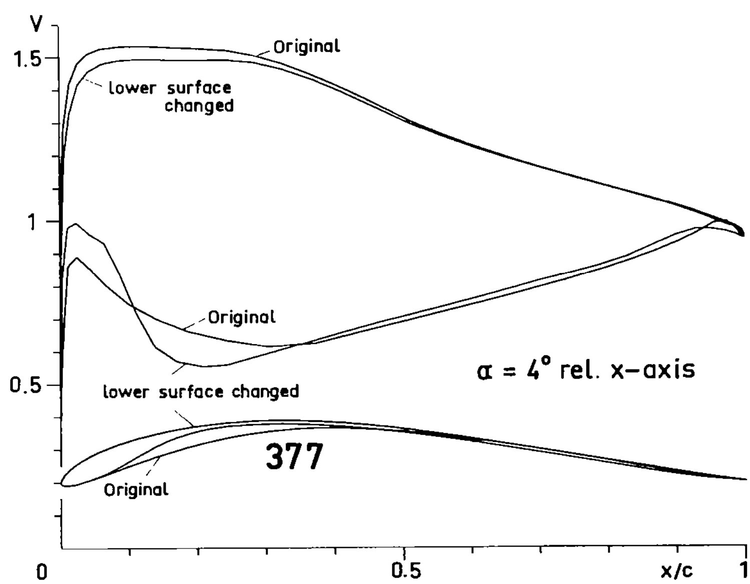


Figure 10.- Comparison of original and modified airfoil 377.

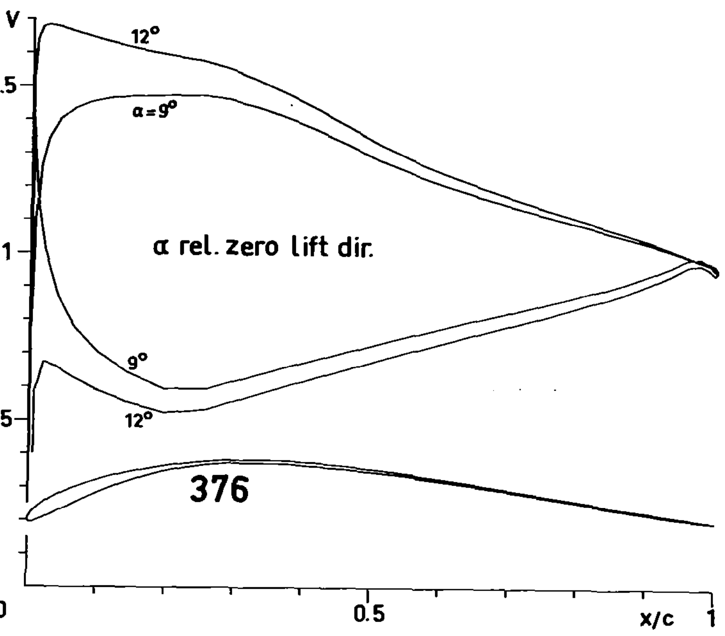


Figure 11.- Velocity distributions for airfoil 376.

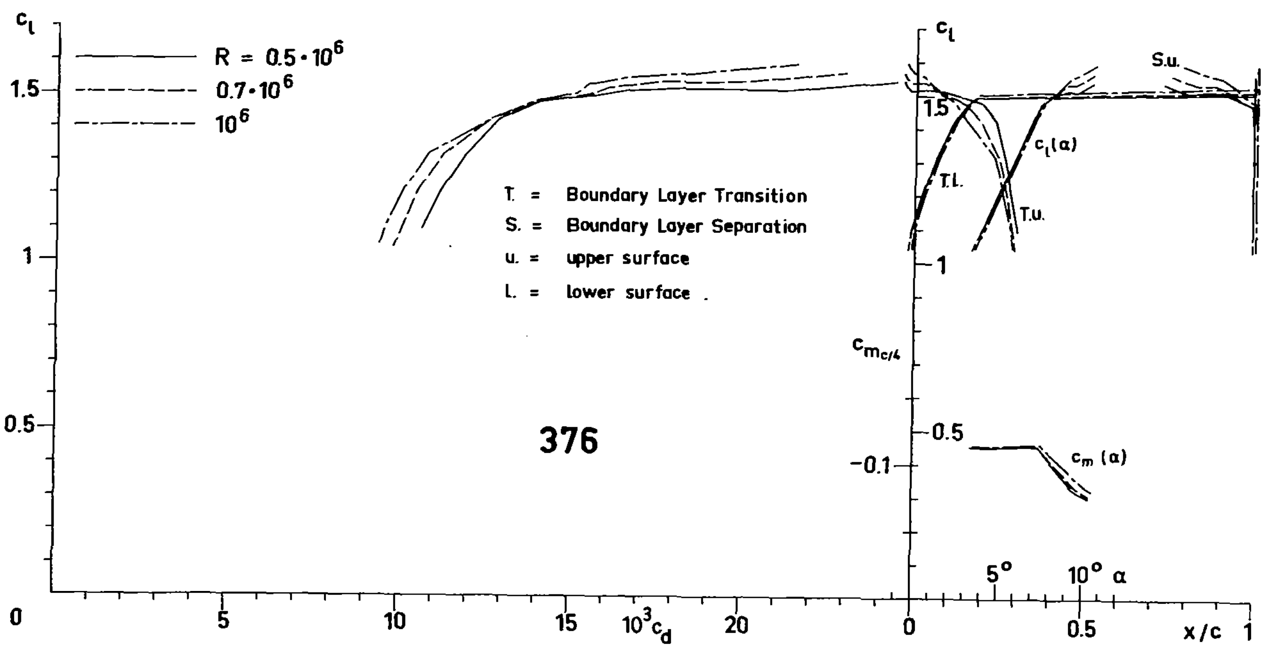


Figure 12.- Theoretical section characteristics for airfoil 376.

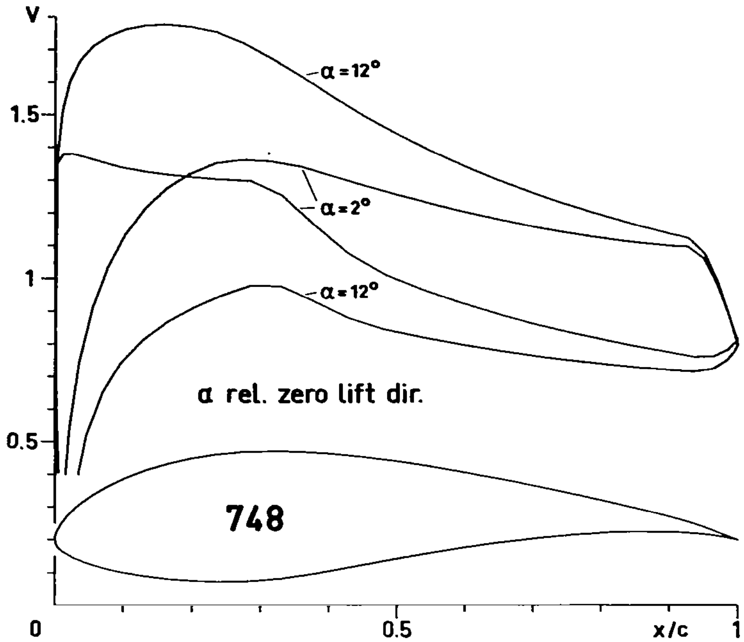


Figure 13.- Velocity distributions for airfoil 748.

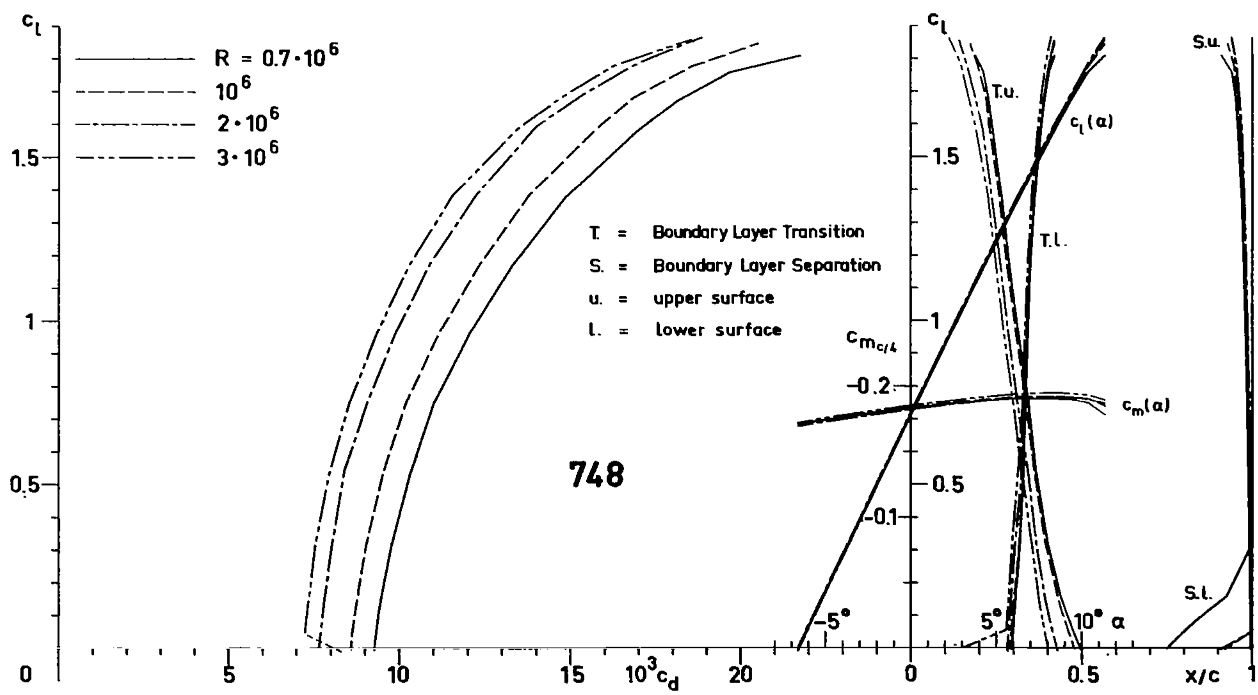


Figure 14.- Theoretical section characteristics for airfoil 748.

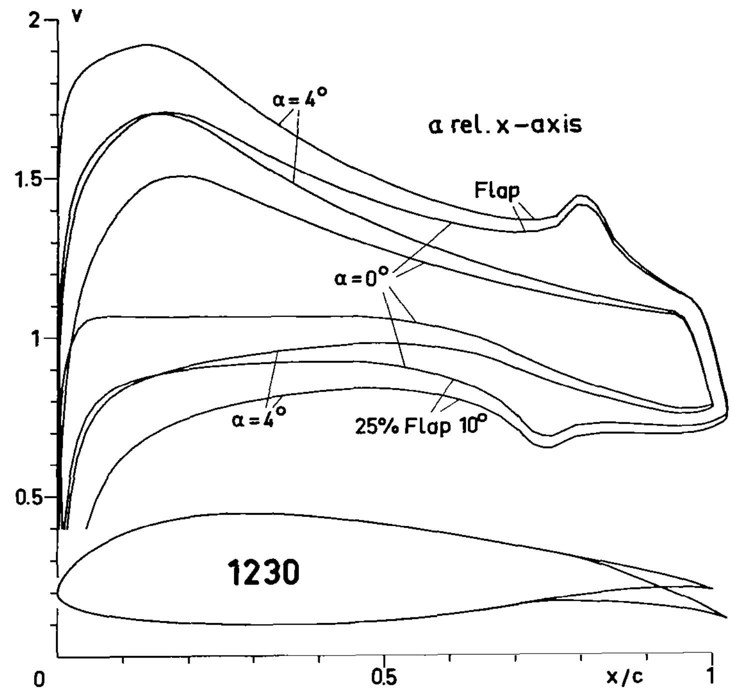


Figure 15.- Velocity distributions for airfoil 1230.

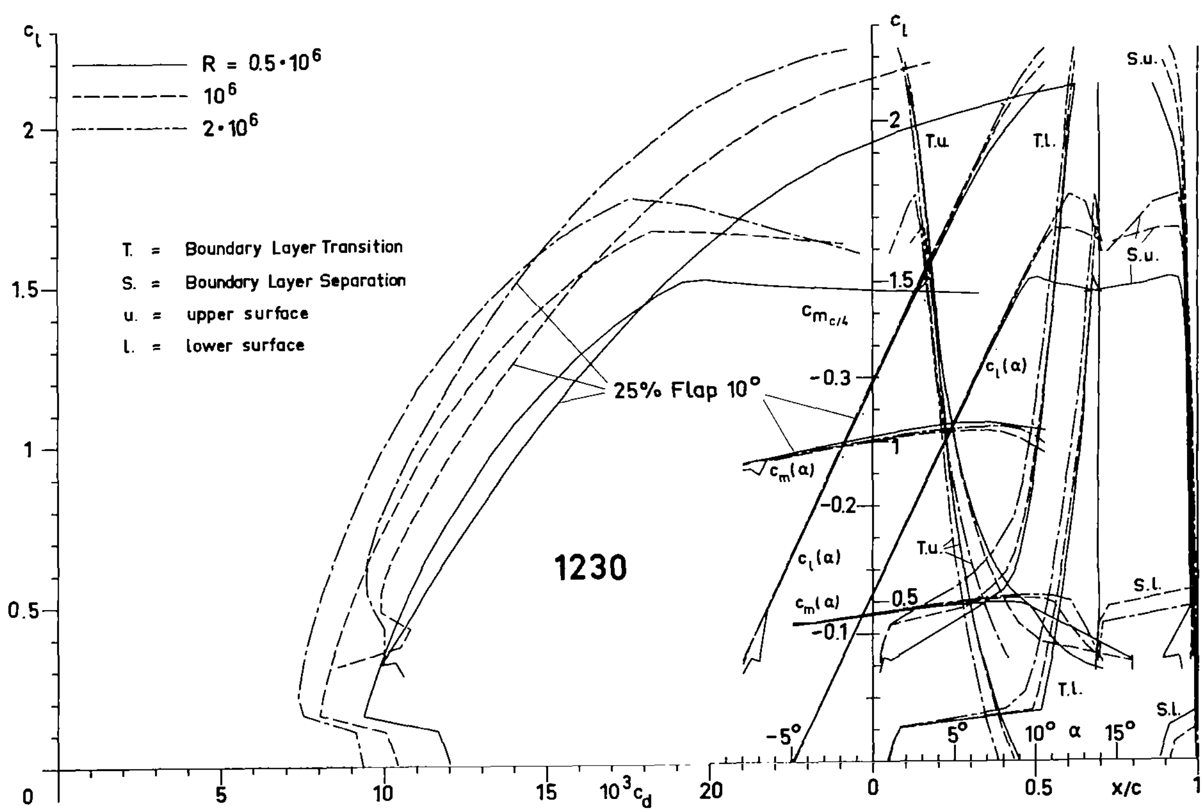


Figure 16.- Theoretical section characteristics for airfoil 1230.

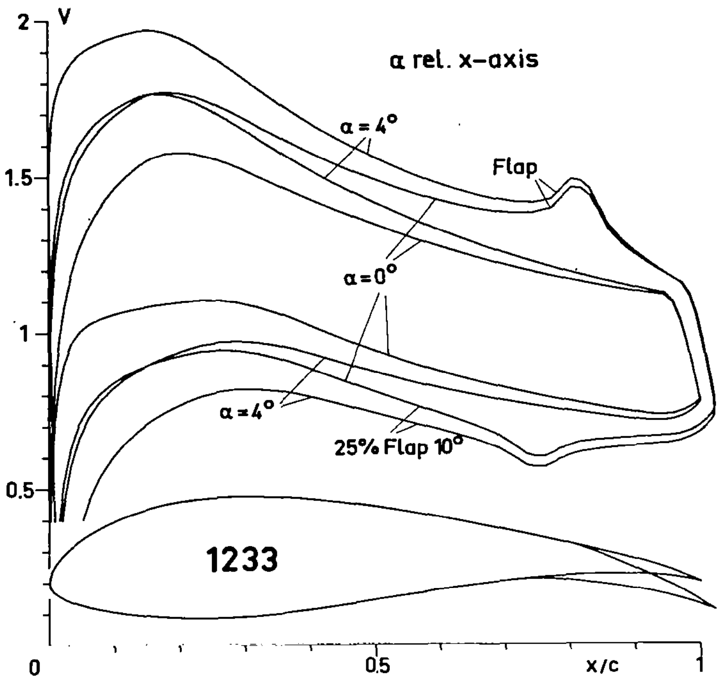


Figure 17.- Velocity distributions for airfoil 1233.

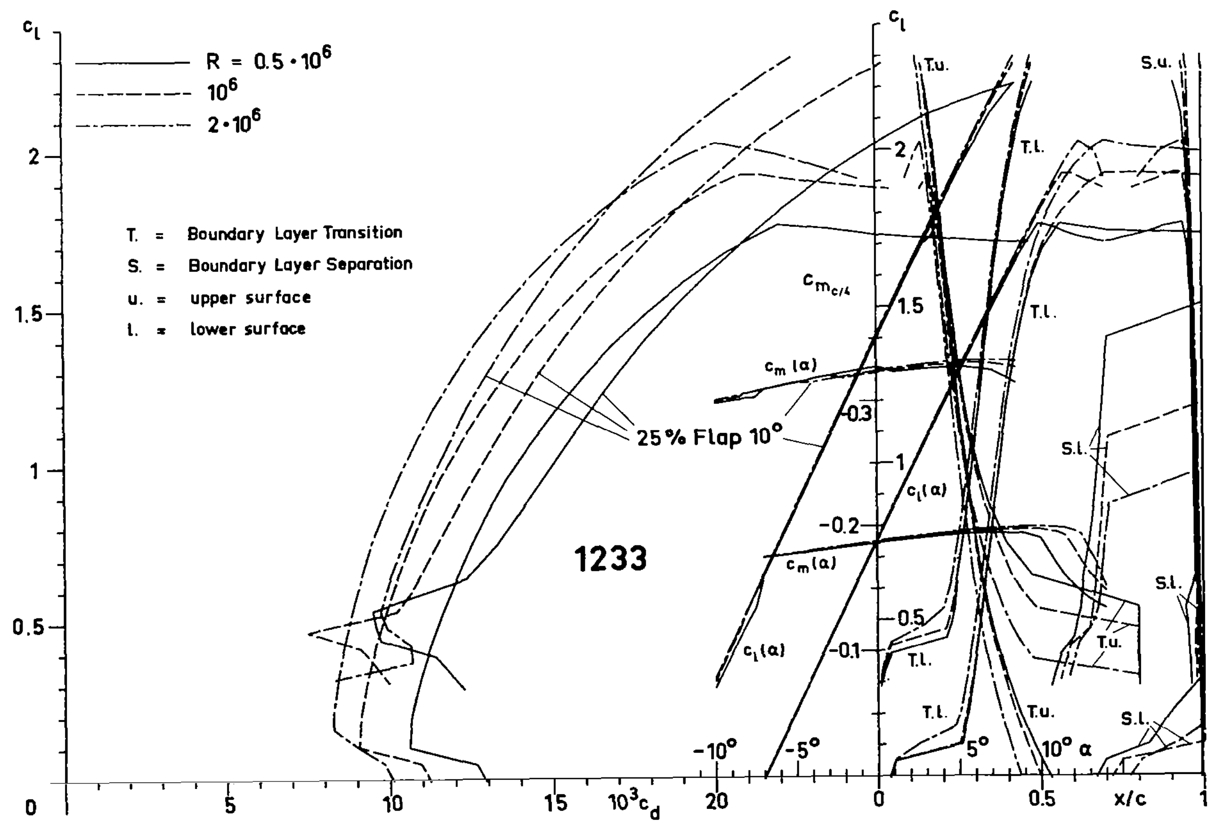


Figure 18.- Theoretical section characteristics for airfoil 1233.

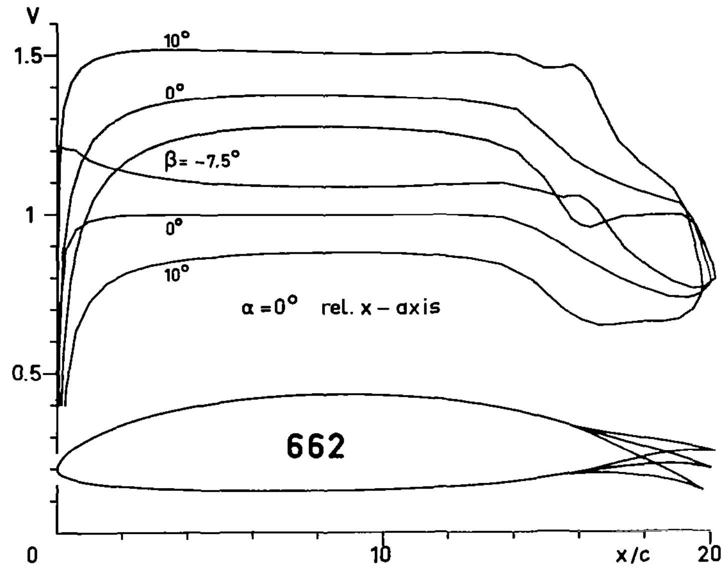


Figure 19.- Velocity distributions for airfoil 662.

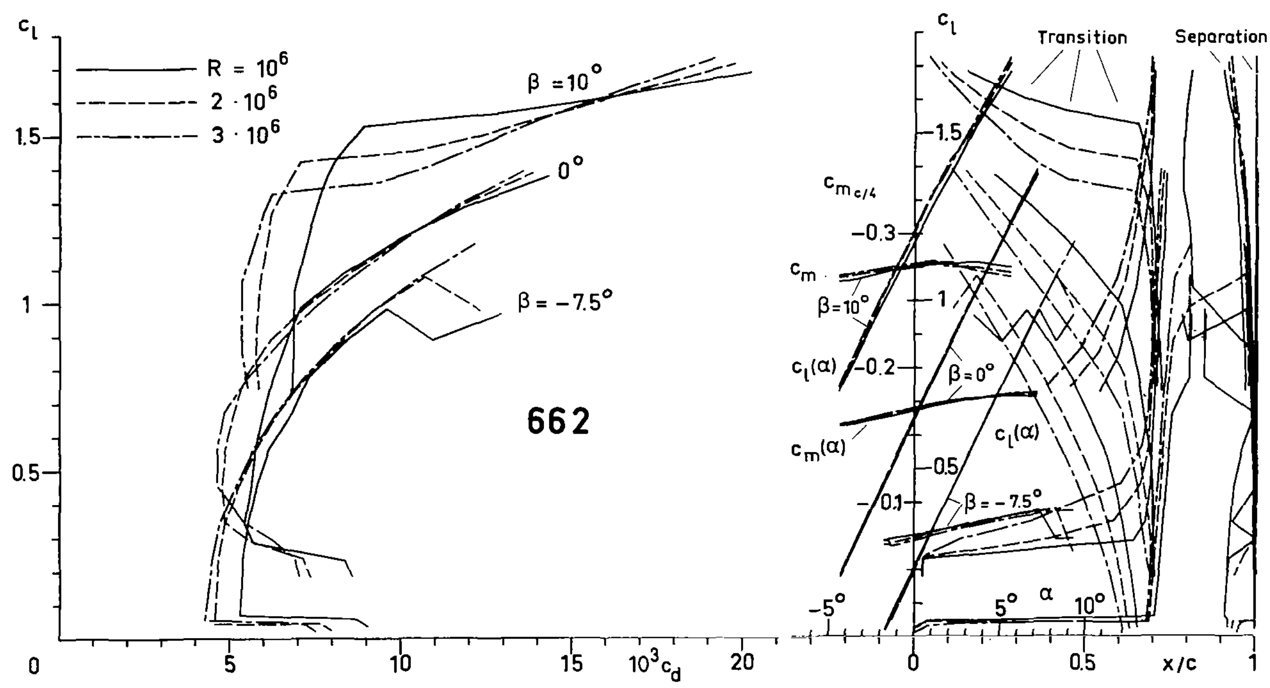


Figure 20.- Theoretical section characteristics for airfoil 662.

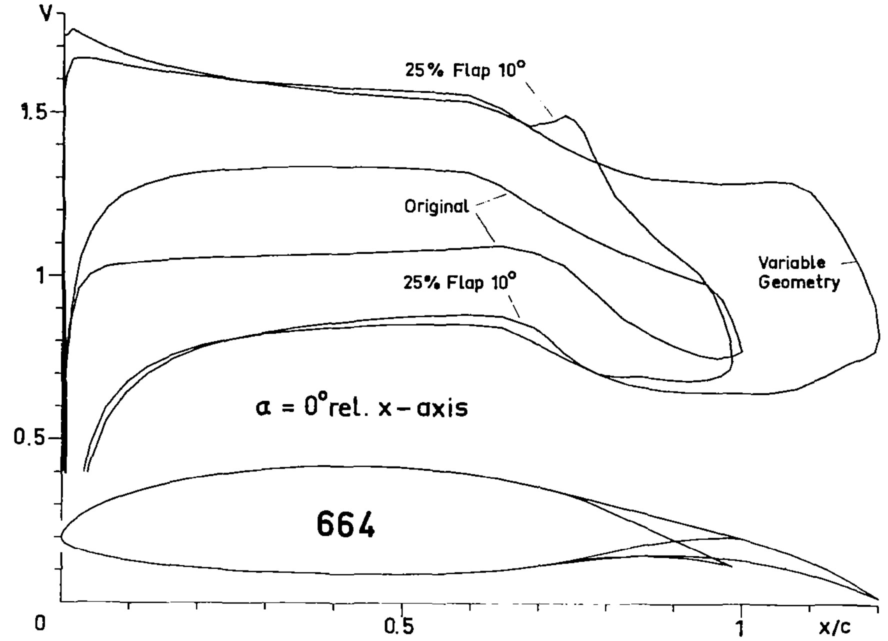


Figure 21.- Velocity distributions for variable geometry airfoil 664.

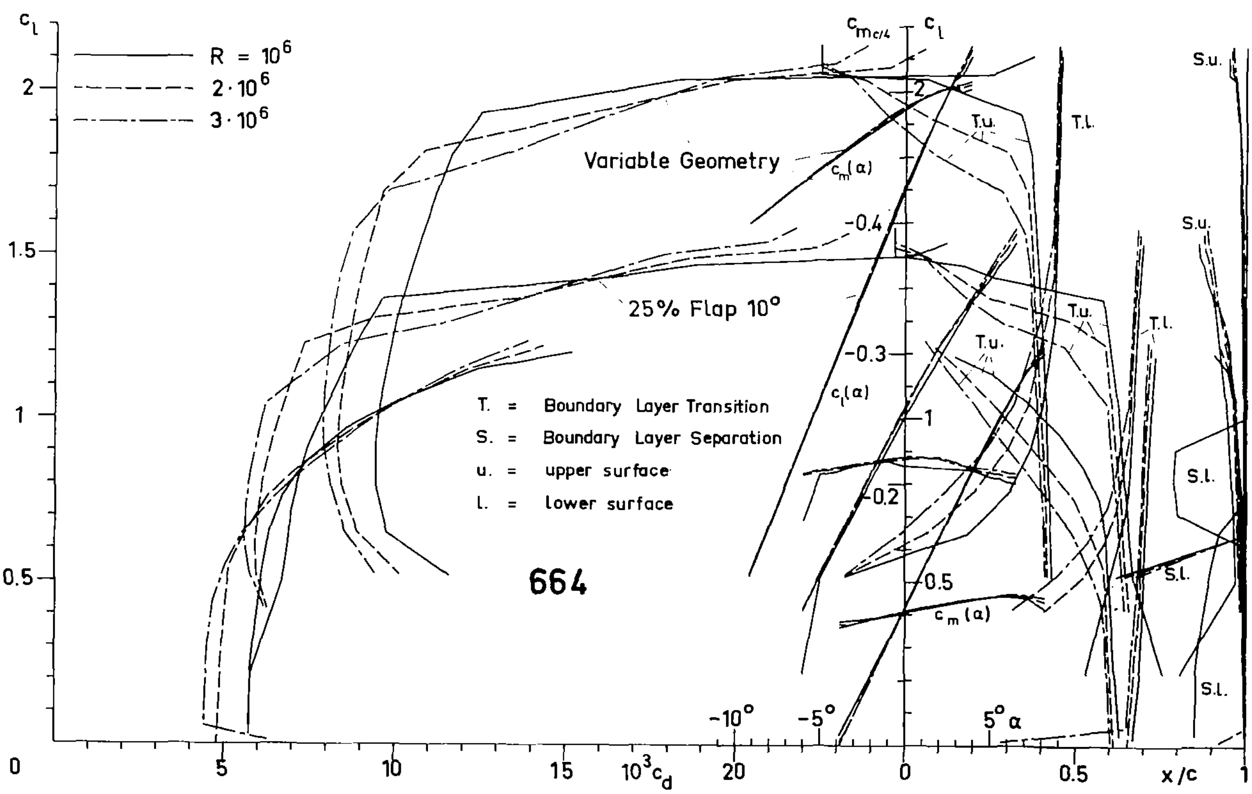


Figure 22.- Theoretical section characteristics for variable geometry airfoil 664.